

CERN -EP 90-79

03 JUL. 1990

c 2

AS



CM-P00056451

EUROPEAN ORGANIZATION FOR NUCLEAR RESEARCH

CERN-EP/90-79

8 June 1990

Search for Scalar Quarks in Z^0 Decays

DELPHI Collaboration

Abstract

A search has been made for pairs of scalar quarks (squarks) produced in e^+e^- annihilations at LEP ($\sqrt{s} \simeq M_{Z^0}$), and decaying into a standard quark and a neutral, non-interacting, stable, massive particle (the Lightest Supersymmetric Particle, LSP). The search has been conducted for differences in the mass of the squark and LSP of $2 \text{ GeV}/c^2$ and above. Up squarks with masses below $42 \text{ GeV}/c^2$ and down squarks below $43 \text{ GeV}/c^2$ were excluded. Six squark flavours degenerate in mass were excluded below $45 \text{ GeV}/c^2$.

(Submitted to Physics Letters B)

P.Abreu¹⁶, W.Adam³⁷, F.Adami²⁸, T.Adye²⁷, G.D.Alexeev¹², J.V.Allaby⁷, P.Allen³⁶, S.Almehed¹⁹,
 F.Alted³⁶, S.J.Alvsvaag⁴, U.Amaldi⁷, E.Anassontzis³, W-D.Apel¹³, B.Asman³², C.Astor Ferreres³⁰,
 J-E.Augustin¹⁵, A.Augustinus⁷, P.Baillon⁷, P.Bambade¹⁵, F.Barao¹⁶, G.Barbiellini³⁴, D.Y.Bardin¹²,
 A.Baroncelli²⁹, O.Barring¹⁹, W.Bartl³⁷, M.J.Bates²⁵, M.Baubillier¹⁸, K-H.Becks³⁹, C.J.Beeston²⁵,
 P.Beilliere⁶, I.Belokopytov³¹, P.Beltran⁹, D.Benedic⁸, J.M.Benloch³⁶, M.Berggren³², D.Bertrand²,
 S.Biagi¹⁷, F.Bianchi³³, J.H.Bibby²⁵, M.S.Bilenky¹², P.Billoir¹⁸, J.Bjarne¹⁹, D.Bloch⁸, P.N.Bogolubov¹²,
 D.Bollini⁵, T.Bolognese²⁸, M.Bonapart²², P.S.L.Booth¹⁷, M.Boratav¹⁸, P.Borgeaud²⁸, H.Borner²⁵,
 C.Bosio²⁹, O.Botner³⁵, B.Bouquet¹⁵, M.Bozzo¹⁰, S.Braibant⁷, P.Branchini²⁹, K.D.Brand³⁹,
 R.A.Brenner¹¹, C.Bricman², R.C.A.Brown⁷, N.Brummer²², J-M.Brunet⁶, L.Bugge²⁴, T.Buran²⁴,
 H.Burmeister⁷, C.Buttar²⁵, J.A.M.A.Buytaert², M.Caccia²⁰, M.Calvi²⁰, A.J.Camacho Rozas³⁰,
 J-E.Campagne⁷, A.Campion¹⁷, T.Camporesi⁷, V.Canale²⁹, F.Cao², L.Carroll¹⁷, C.Caso¹⁰, E.Castelli³⁴,
 M.V.Castillo Gimenez³⁶, A.Cattai⁷, F.R.Cavallo⁵, L.Cerrito²⁹, P.Charpentier⁷, P.Checchia²⁶,
 G.A.Chelkov¹², L.Chevalier²⁸, P.Chliapnikov³¹, V.Chorowicz¹⁸, R.Cirio³³, M.P.Clara³³,
 J.L.Contreras³⁶, R.Contri¹⁰, G.Cosme¹⁵, F.Couchot¹⁵, H.B.Crawley¹, D.Crennell²⁷, M.Cresti²⁶,
 G.Crosetti¹⁰, N.Crosland²⁵, M.Crozon⁶, J.Cuevas Maestro³⁰, S.Czellar¹¹, S.Dagoret¹⁵,
 E.Dahl-Jensen²¹, B.Dalmagne¹⁵, M.Dam⁷, G.Damgaard²¹, G.Darbo¹⁰, E.Daubie², M.Davenport⁷,
 P.David¹⁸, A.De Angelis³⁴, M.De Beer²⁸, H.De Boeck², W.De Boer¹³, C.De Clercq²,
 M.D.M.De Fez Laso³⁶, N.De Groot²², C.De La Vaissiere¹⁸, B.De Lotto³⁴, A.De Min²⁰, C.Defoix⁶,
 D.Delikaris⁷, P.Delpierre⁶, N.Demaria³³, L.Di Ciaccio²⁹, A.N.Diddens²², H.Dijkstra⁷, F.Djama⁸,
 J.Dolbeau⁶, K.Doroba³⁸, M.Dracos⁸, J.Drees³⁹, M.Dris²³, W.Dulinski⁸, R.Dzhelyadin³¹,
 D.N.Edwards¹⁷, L-O.Eek³⁵, P.A.-M.Eerola¹¹, T.Ekelof³⁵, G.Ekspong³², J-P.Engel⁸, V.Falaleev³¹,
 A.Fenyuk³¹, M.Fernandez Alonso³⁰, A.Ferrer³⁶, S.Ferroni¹⁰, T.A.Filippas²³, A.Firestone¹, H.Foeth⁷,
 E.Fokitis²³, F.Fontanelli¹⁰, H.Forsbach³⁹, B.Franek²⁷, K.E.Fransson³⁵, P.Frenkiel⁶, D.C.Fries¹³,
 R.Fruhwrith³⁷, F.Fulda-Quenzer¹⁵, H.Furstenau¹³, J.Fuster⁷, J.M.Gago¹⁶, G.Galeazzi²⁶, D.Gamba³³,
 U.Gasparini²⁶, P.Gavillet⁷, S.Gawne¹⁷, E.N.Gazis²³, P.Giacomelli⁵, K-W.Glitza³⁹, R.Gokieli¹⁸,
 V.M.Golovatyuk¹², A.Goobar³², G.Gopal²⁷, M.Gorski³⁸, V.Gracco¹⁰, A.Grant⁷, F.Grard²,
 E.Graziani²⁹, M-H.Gros¹⁵, G.Grosdidier¹⁵, B.Grossetete¹⁸, S.Gumenyuk³¹, J.Guy²⁷, F.Hahn³⁹,
 M.Hahn¹³, S.Haider⁷, Z.Hajduk²², A.Hakansson¹⁹, A.Hallgren³⁵, K.Hamacher³⁹,
 G.Hamel De Monchenault²⁸, F.J.Harris²⁵, B.Heck⁷, I.Herbst³⁹, J.J.Hernandez³⁶, P.Herquet², H.Herr⁷,
 E.Higon³⁶, H.J.Hilke⁷, T.Hofmohl³⁸, R.Holmes¹, S-O.Holmgren³², J.E.Hooper²¹, M.Houlden¹⁷,
 J.Hrubic³⁷, P.O.Hulth³², K.Hultqvist³², D.Husson⁸, B.D.Hyams⁷, P.Ioannou³, P-S.Iversen⁴,
 J.N.Jackson¹⁷, P.Jalocha¹⁴, G.Jarlskog¹⁹, P.Jarry²⁸, B.Jean-Marie¹⁵, E.K.Johansson³², M.Jonker⁷,
 L.Jonsson¹⁹, P.Juillot⁸, R.B.Kadyrov¹², G.Kalkanis³, G.Kalmus²⁷, G.Kantardjian⁷, F.Kapusta¹⁸,
 P.Kapusta¹⁴, S.Katsanevas³, E.C.Katsoufis²³, R.Keranen¹¹, J.Kesteman², B.A.Khomenko¹², B.King¹⁷,
 N.J.Kjaer²¹, H.Klein⁷, W.Klemp⁷, A.Klovning⁴, P.Kluit², J.H.Koehne¹³, B.Koene²², P.Kokkinias⁹,
 M.Kopf¹³, M.Koratzinos⁷, K.Korcyll¹⁴, A.V.Korytov¹², B.Korzen⁷, C.Kourkoumelis³, T.Kreuzberger³⁷,
 J.Krolikowski³⁸, U.Kruener-Marquis³⁹, W.Krupinski¹⁴, W.Kucewicz²⁰, K.Kurvinen¹¹, M.I.Laakso¹¹,
 C.Lambropoulos⁹, J.W.Lamsa¹, L.Lanceri³⁴, V.Lapin³¹, J-P.Laugier²⁸, R.Lauhakangas¹¹,
 P.Laurikainen¹¹, G.Leder³⁷, F.Ledroit⁶, J.Lemonne², G.Lenzen³⁹, V.Lepeltier¹⁵, A.Letessier-Selvon¹⁸,
 E.Lieb³⁹, E.Lillestol⁷, E.Lillethun⁴, J.Lindgren¹¹, I.Lippi²⁶, R.Llosa³⁶, B.Loerstad¹⁹, M.Lokajicek¹²,
 J.G.Loken²⁵, M.A.Lopez Aguera³⁰, A.Lopez-Fernandez¹⁵, D.Loukas⁹, J.J.Lozano³⁶, R.Lucock²⁷,
 B.Lund-Jensen³⁵, P.Lutz⁶, L.Lyons²⁵, G.Maehlum⁷, J.Maillard⁶, A.Maltezos⁹, F.Mandl³⁷, J.Marco³⁰,
 J-C.Marin⁷, A.Markou⁹, L.Mathis⁶, C.Matteuzzi²⁰, G.Matthiae²⁹, M.Mazzucato²⁶, M.Mc Cubbin¹⁷,
 R.Mc Kay¹, E.Menichetti³³, C.Meroni²⁰, W.T.Meyer¹, W.A.Mitaroff³⁷, G.V.Mitselmakher¹²,
 U.Mjoernmark¹⁹, T.Moa³², R.Moeller²¹, K.Moenig³⁹, M.R.Monge¹⁰, P.Morettini¹⁰, H.Mueller¹³,
 H.Muller⁷, G.Myatt²⁵, F.Naraghi¹⁸, U.Nau-Korzen³⁹, F.L.Navarria⁵, P.Negri²⁰, B.S.Nielsen²¹,
 V.Nikolaenko³¹, V.Obratsov³¹, R.Orava¹¹, A.Ouraou²⁸, R.Pain¹⁸, H.Palka¹⁴, T.Papadopoulou²³,
 L.Pape⁷, P.Pasini⁵, A.Pasleri²⁹, M.Pegoraro²⁶, V.Perevozchikov³¹, M.Pernicka³⁷, M.Pimenta¹⁶,
 O.Pingot², C.Pinori²⁶, A.Pinsent²⁵, M.E.Pol¹⁶, B.Poliakov³¹, G.Polok¹⁴, P.Poropat³⁴, P.Privitera⁵,
 A.Pullia²⁰, J.Pyyhtia¹¹, A.A.Rademakers²², D.Radojicic²⁵, S.Ragazzi²⁰, W.H.Range¹⁷, P.N.Ratoff²⁵,
 A.L.Read²⁴, N.G.Redaeli²⁰, M.Regler³⁷, D.Reid¹⁷, P.B.Renton²⁵, L.K.Resvanis³, F.Richard¹⁵,
 J.Ridky¹², G.Rinaudo³³, I.Roditi⁷, A.Romero³³, P.Ronchese²⁶, E.I.Rosenberg¹, U.Rossi⁵, E.Rosso⁷,
 P.Roudeau¹⁵, T.Rovelli⁵, V.Ruhlmann²⁸, A.Ruiz³⁰, H.Saarikko¹¹, Y.Sacquin²⁸, E.Sanchez³⁶,
 J.Sanchez³⁶, E.Sanchis³⁶, M.Sannino¹⁰, M.Schaeffer⁸, H.Schneider¹³, F.Scuri³⁴, A.Sebastia³⁶,
 A.M.Segar²⁵, R.Sekulin²⁷, M.Sessa³⁴, G.Sette¹⁰, R.Seufert¹³, R.C.Shellard⁷, P.Siegrist²⁸, S.Simonetti¹⁰,
 F.Simonetto²⁶, A.N.Sissakian¹², T.B.Skaali²⁴, J.Skeens¹, G.Skjevling²⁴, G.Smadja²⁸, N.E.Smirnov³¹,
 G.R.Smith²⁷, R.Sosnowski³⁸, K.Spang²¹, T.Spasoff¹², E.Spiriti²⁹, S.Squarcia¹⁰, H.Staek³⁹,
 C.Stanescu²⁹, G.Stavropoulos⁹, F.Stichelbaut², A.Stocchi²⁰, J.Strauss³⁷, R.Strub⁸, C.J.Stubenrauch⁷,

M.Szczekowski³⁸, M.Szeptycka³⁸, P.Szymanski³⁸, S.Tavernier², G.Theodosiou⁹, A.Tilquin⁶, J.Timmermans²², V.G.Timofeev¹², L.G.Tkatchev¹², D.Z.Toet²², A.K.Topphol⁴, L.Tortora²⁹, D.Treille⁷, U.Trevisan¹⁰, G.Tristram⁶, C.Troncon²⁰, E.N.Tsyganov¹², M.Turala¹⁴, R.Turchetta⁸, M-L.Turluer²⁸, T.Tuuva¹¹, I.A.Tyapkin¹², M.Tyndel²⁷, S.Tzamarias⁷, F.Udo²², S.Ueberschaer³⁹, V.A.Uvarov³¹, G.Valenti⁵, E.Vallazza³³, J.A.Valls Ferrer³⁶, G.W.Van Apeldoorn²², P.Van Dam²², W.K.Van Doninck², N.Van Eijndhoven⁷, C.Vander Velde², J.Varela¹⁶, P.Vaz¹⁶, G.Vegni²⁰, M.E.Veitch²⁵, J.Velasco³⁶, L.Ventura²⁶, W.Venus²⁷, F.Verbeure², L.S.Vertogradov¹², L.Vibert¹⁸, D.Vilanova²⁸, N.K.Vishnevskiy³¹, E.V.Vlasov³¹, A.S.Vodopyanov¹², M.Vollmer³⁹, G.Voulgaris³, M.Voutilainen¹¹, V.Vrba¹², H.Wahlen³⁹, C.Walck³², F.Waldner³⁴, M.Wayne¹, P.Weilhammer⁷, J.Werner³⁹, A.M.Wetherell⁷, J.H.Wickens², J.Wikne²⁴, W.S.C.Williams²⁵, M.Winter⁸, D.Wormald²⁴, G.Wormser¹⁵, K.Woschnagg³⁵, N.Yamdagni³², P.Yepes²², A.Zaitsev³¹, A.Zalewska¹⁴, P.Zalewski³⁸, P.I.Zarubin¹², E.Zevgolatakos⁹, G.Zhang³⁹, N.I.Zimin¹², R.Zitoun¹⁸, R.Zukanovich Funchal⁶, G.Zumerle²⁶, J.Zuniga³⁶

¹Ames Laboratory and Department of Physics, Iowa State University, Ames IA 50011, USA

²Physics Department, Univ. Instelling Antwerpen, Universiteitsplein 1, B-2610 Wilrijk, Belgium and IIHE, ULB-VUB, Pleinlaan 2, B-1050 Brussels, Belgium

and Service de Phys. des Part. Elém., Faculté des Sciences, Université de l'Etat Mons, Av. Maistriau 19, B-7000 Mons, Belgium

³Physics Laboratory, University of Athens, Solonos Str. 104, GR-10680 Athens, Greece

⁴Department of Physics, University of Bergen, Allégaten 55, N-5007 Bergen, Norway

⁵Dipartimento di Fisica, Università di Bologna and INFN, Via Irnerio 46, I-40126 Bologna, Italy

⁶Collège de France, Lab. de Physique Corpusculaire, 11 pl. M. Berthelot, F-75231 Paris Cedex 05, France

⁷CERN, CH-1211 Geneva 23, Switzerland

⁸Division des Hautes Energies, CRN - Groupe DELPHI, B.P. 20 CRO, F-67037 Strasbourg Cedex, France

⁹Greek Atomic Energy Commission, Nucl. Research Centre Demokritos, P.O. Box 60228, GR-15310 Aghia Paraskevi, Greece

¹⁰Dipartimento di Fisica, Università di Genova and INFN, Via Dodecaneso 33, I-16146 Genova, Italy

¹¹Dept. of High Energy Physics, University of Helsinki, Siltavuorenpenger 20 C, SF-00170 Helsinki 17, Finland

¹²Joint Institute for Nuclear Research, Dubna, Head Post Office, P.O. Box 79, 101 000 Moscow, USSR.

¹³Institut für Experimentelle Kernphysik, Universität Karlsruhe, Postfach 6980, D-7500 Karlsruhe 1, FRG

¹⁴High Energy Physics Laboratory, Institute of Nuclear Physics, Ul. Kawory 26 a, PL-30055 Krakow 30, Poland

¹⁵Université de Paris-Sud, Lab. de l'Accélérateur Linéaire, Bat 200, F-91405 Orsay, France

¹⁶LIP, Av. Elias Garcia 14 - 1e, P-1000 Lisbon Codex, Portugal

¹⁷Department of Physics, University of Liverpool, P.O. Box 147, GB - Liverpool L69 3BX, UK

¹⁸LPNHE, Universités Paris VI et VII, Tour 33 (RdC), 4 place Jussieu, F-75230 Paris Cedex 05, France

¹⁹Department of Physics, University of Lund, Sölvegatan 14, S-22363 Lund, Sweden

²⁰Dipartimento di Fisica, Università di Milano and INFN, Via Celoria 16, I-20133 Milan, Italy

²¹Niels Bohr Institute, Blegdamsvej 17, DK-2100 Copenhagen 0, Denmark

²²NIKHEF-H, Postbus 41882, NL-1009 DB Amsterdam, The Netherlands

²³National Technical University, Physics Department, Zografou Campus, GR-15773 Athens, Greece

²⁴Physics Department, University of Oslo, Blindern, N-1000 Oslo 3, Norway

²⁵Nuclear Physics Laboratory, University of Oxford, Keble Road, GB - Oxford OX1 3RH, UK

²⁶Dipartimento di Fisica, Università di Padova and INFN, Via Marzolo 8, I-35131 Padua, Italy

²⁷Rutherford Appleton Laboratory, Chilton, GB - Didcot OX11 0QX, UK

²⁸CEN-Saclay, DPhPE, F-91191 Gif-sur-Yvette Cedex, France

²⁹Istituto Superiore di Sanità, Ist. Naz. di Fisica Nucl. (INFN), Viale Regina Elena 299, I-00161 Rome, Italy and Dipartimento di Fisica, Università di Roma II and INFN, Tor Vergata, I-00173 Rome.

³⁰Facultad de Ciencias, Universidad de Santander, av. de los Castros, E - 39005 Santander, Spain

³¹Inst. for High Energy Physics, Serpukov P.O. Box 35, Protvino, (Moscow Region), USSR.

³²Institute of Physics, University of Stockholm, Vanadisvägen 9, S-113 46 Stockholm, Sweden

³³Dipartimento di Fisica Sperimentale, Università di Torino and INFN, Via P. Giuria 1, I-10125 Turin, Italy

³⁴Dipartimento di Fisica, Università di Trieste and INFN, Via A. Valerio 2, I-34127 Trieste, Italy

and Istituto di Fisica, Università di Udine, I-33100 Udine, Italy

³⁵Department of Radiation Physics, University of Uppsala, P.O. Box 535, S-751 21 Uppsala, Sweden

³⁶Inst. de Fisica Corpuscular IFIC, Centro Mixto Univ. de Valencia-CSIC, Avda. Dr. Moliner 50, E-46100 Burjassot (Valencia), Spain

³⁷Institut für Hochenergiephysik, Österreich Akad. d. Wissensch., Nikolsdorfergasse 18, A-1050 Vienna, Austria

³⁸Inst. Nuclear Studies and, University of Warsaw, Ul. Hoza 69, PL-00681 Warsaw, Poland

³⁹Fachbereich Physik, University of Wuppertal, Postfach 100 127, D-5600 Wuppertal 1, FRG

1 Introduction

A large number of high energy e^+e^- annihilations have been recorded during the 1989 running period of LEP, the CERN electron-positron collider. Novel strategies that use the large statistics around the Z^0 resonance and rely on the clean machine conditions can be applied in searching for new phenomena.

This paper reports a search, using the DELPHI detector, for new heavy unstable charged particles which are pair produced in Z^0 decays, and decay immediately producing a neutral and non-interacting stable particle together with a standard quark. Decays of this type are to be expected in some theories beyond the Standard Model. In particular, supersymmetric models predict reactions of the type

$$e^+e^- \rightarrow Z^0 \rightarrow \tilde{q}\tilde{\bar{q}} \rightarrow \tilde{\chi}^0 q \tilde{\chi}^0 \bar{q}, \quad (1)$$

where the scalar supersymmetric partners \tilde{q} and $\tilde{\bar{q}}$ of the quark and antiquark decay into the undetected lightest supersymmetric particle (LSP) $\tilde{\chi}^0$ and a quark q . Previous searches for these types of processes were based on the signature of a momentum imbalance appearing either as acollinear jets or as events with large missing transverse momentum ([1]-[5]). Such approaches require a large difference between the mass of the charged decaying particle and the mass of the neutral invisible particle. In the case of a *heavy* invisible object, close in mass to the decaying particle, the experimental signature changes from a clearly distinguishable acollinear jet topology to events of small visible energy. At hadron colliders these events have low trigger efficiencies and high backgrounds due to soft processes. At e^+e^- colliders they are contaminated by two-photon interactions and machine backgrounds.

The present search was based on two different analysis. The *first* one applies to heavy invisible objects and is new. It utilises e^+e^- annihilations at center-of-mass energies around the Z^0 boson mass. The cross section of the new process is expected to follow the standard line shape of the Z^0 boson and, thus, to exceed on the peak the cross section due to s -channel photon exchange by several orders of magnitude. Data points at center-of-mass energies around the Z^0 pole are a direct experimental check of the estimates for the backgrounds which are decoupled from the Z^0 . Hence the rates of these background events may be reliably determined. The *second* analysis which follows previous works ([1]-[2]), is based on searching for acollinear jets and puts limits for LSP masses less than about half of the squark mass. Most of the paper is devoted to an explanation of the new approach applied in the first analysis.

The squarks \tilde{q} and $\tilde{\bar{q}}$ of Eq.(1) couple to the Z^0 analogously to the corresponding fermionic quark fields and the expected cross sections are calculable for each flavour and helicity [6]. In case of low squark masses, the cross sections are at the level of three nanobarns for single flavours and they can contribute to the hadronic or to the invisible width of the Z^0 (depending on the mass of the LSP). The phase space factor $\beta^3 = (1 - 4M_{\tilde{q}}^2/s)^{3/2}$ affects the rates over a wide portion of the kinematically accessible region.

In both analysis presented here, each squark was assumed to decay immediately with a 100 % branching ratio into a LSP (heavy gluino assumed) and a quark. Only mass differences between the squark and the LSP above 2 GeV were investigated, since closer masses lead to theoretical uncertainties in the multiplicities of the fragmentation of low energy quark-antiquark systems. Some characteristics of the expected signal are shown in Figure 1 in which the distributions of the total charged energy are plotted

for three combinations of the masses of the scalar quarks and the heavy LSP. In the first analysis the search was concentrated on events having a total charged energy smaller than 20 GeV whereas in case of LSP masses less than half of the squark mass, the total charged energy is well within the distribution from the standard quarks and events with visible energy larger than 15 GeV were considered.

2 The detector and trigger arrangement

The components of DELPHI [7] relevant for this work are the Time Projection Chamber (TPC), the Inner and the Outer Detectors (ID, OD), and the Small Angle Tagger (SAT).

The ID is a cylindrical drift chamber covering the polar angle range 30° to 150° . It contains five trigger layers giving information about the cylindrical $r\phi$ and longitudinal z coordinates at the radius of 22 cm around the beam axis. The jet chamber section providing the $r\phi$ coordinates of 24 points. The TPC is a cylinder with an inner radius of 30 cm, outer radius of 122 cm and with anode wires at a distance of 134 cm from the central high voltage plane at $z = 0$. The TPC records 16 space points (for polar angles of 40° to 140°), z -coordinates derived from the drift time onto the wires and $r\phi$ coordinates from the circular pad rows behind the anode wires. At least six space points are registered down to polar angles of 24° . The OD is a cylindrical tracking device consisting of 24 aluminium drift tube assemblies in five layers at a radius of 198-208 cm. It provides five accurate $r\phi$ space points and three fast z coordinates per track at polar angles between 50° and 130° and contributed also to the track trigger. The SAT calorimeters cover polar angles of 43 to 135 mrad in the beam directions. They consist of scintillating fibres embedded in a lead absorber

and they measure the integrated luminosity by monitoring the rate of small angle Bhabha scattering. Details of the luminosity measurement are given in Ref. [8].

The component of the DELPHI trigger that is most important for this analysis is the barrel track trigger consisting of the coincidence of back to back OD quadrants with any signal from the ID trigger layers. The information about all the trigger components was included in the data on an event-to-event basis, and the efficiency of this particular trigger could be measured by using the redundancy of the independent barrel trigger information from the scintillator layer behind the first 5 radiation lengths of the barrel electromagnetic calorimeter combined with the 172 time of flight counters outside the solenoid. Figure 2 shows the trigger efficiency as a function of the visible charged energy calculated from the data.

3 Event selection for heavy LSPs

Events used in this analysis contain at least one reconstructed charged track with a momentum larger than $0.5 \text{ GeV}/c$, a radial impact parameter less than 15 cm and a longitudinal distance z from the interaction point less than 30 cm . These selection criteria were chosen to include events to measure the machine backgrounds, as discussed later. The detector conditions were checked for the detector parts which were necessary for the reconstruction and the trigger. After this run selection 13500 events remained, corresponding to an integrated luminosity of 330 nb^{-1} divided into ten samples at center-of-mass energies between 88.28 and 95.04 GeV.

In each event, the average impact distance in the z -direction, \hat{z} , and its variance, $\sigma(z)$, were calculated for the selected charged particle tracks.

The candidates were selected by requiring

1. a total visible charged energy less than 20 GeV,
2. more than two charged particles (this criterion rejected cosmic triggers, beam halo tracks, and leptonic Z^0 decays, including a large fraction of the tau pairs, but had a high efficiency for signal events, because the average charged multiplicity in them is always larger than five),
3. $|\hat{z}| < 4$ cm (to reject events that are not at the expected interaction point),
4. $\sigma(z) < 6$ cm (to reject events with an ill defined vertex),
5. $|\cos(\theta_{thrust})| < 0.8$, where θ_{thrust} is the polar angle of the thrust axis with respect to the beam (to reject most two photon interactions),
6. all tracks to have at angles greater than 25° to the beam axis (to veto events oriented very close to the beam direction),
7. energy in the SAT smaller than 4 GeV (to veto two photon candidates and machine backgrounds).

After the selections the sample contained 284 events. It was checked by scanning that the general features of the events were those expected from a combination of two photon events, Z^0 decays with low reconstructed charged energy and events due to machine backgrounds. Most of the off momentum tracks and the beam-gas or beam-wall interactions were rejected by the vertex criteria described above. The reference interval $5 < |\hat{z}| < 30$ cm was used to estimate the remaining beam associated background and its uncertainty. The 390 events in this interval were found to be uniformly distributed in the variable \hat{z} within statistics. By

extrapolating the event density to the vertex interval $|\hat{z}| < 4 \text{ cm}$, a background of 62 ± 3 (stat.) events was estimated. The background rate turned out to be stable from machine fill to machine fill within the relatively poor statistics (often less than 10 events per fill); to take into account possible variations, a 30 % systematic error was added in quadrature with the statistical error. This background was subtracted from the 284 selected events in the subsequent analysis. The number of selected events at each energy was normalized to the SAT measured luminosity to give the measured cross sections which are presented as a function of the center-of-mass energy in Figure 3.

The data of Figure 3 are taken to be the sum of a resonance-shaped contribution due to remaining Z^0 decays and a slowly energy dependent contribution due to the two photon events, that satisfy the selection criteria.

4 Expected signal and search limits in the case of a heavy LSP

A high statistics sample of Monte Carlo events was generated with 1st order radiative corrections, quark fragmentation according to the Lund 6.3 parton shower model [9] and with the detailed simulation of the detector (Ref. [10] shows the general properties of the hadronic Z^0 decays). This was used to estimate the contribution from standard hadronic Z^0 decays (reconstructed only partially due to either a very forward-backward event axis or high neutral content), and from decays into $\tau\bar{\tau}$ pairs. The result was that (0.75 ± 0.25) % of the standard Z^0 decays satisfy the selection criteria. The 0.25 % systematic error was mainly due to uncertainties in the angular dependence of the trigger efficiency. The dependence of the tails of the charged energy distribution on the fragmentation model

was investigated by comparing the α_s^2 matrix element Monte Carlo model with string fragmentation in Lund 6.3 and found to be negligible. These remaining Z^0 's were assumed to be distributed according to the line shape and were normalised to the peak cross section measured in Ref. [8]. Their contribution at the peak is equal to $0.23 \pm 0.07 \text{ nb}$.

The measured cross section for all Z^0 associated processes was estimated by fitting to Figure 3 a Z^0 line shape [8] with a free normalization (representing the remaining standard Z^0 plus possible nonstandard Z^0 decays) plus a constant term (representing the two-photon contribution). The fit had $\chi^2/D.O.F. = 7.9/8$ (Figure 3). The expected background due to the standard Z^0 decays as estimated above was then subtracted from the result. The remaining nonstandard signal associated with the Z^0 , for example due to process (1) was $(-0.09 \pm 0.14) \text{ nb}$ on the peak, This corresponds to -20 ± 32 events integrated over the whole energy interval. The remaining constant background was $0.56 \pm 0.09 \text{ nb}$. The upper limit for a physical, i.e. positive cross section, associated to nonstandard Z^0 decays was determined by excluding 95% of the probability density (Gaussian) in the region of positive cross sections (Ref. [11]). The limit was 0.23 nb , corresponding to 52 events. This number of events was used for deriving the search limits reported below.

The expected rate of the signal events depends on their production cross section, trigger efficiency and selection efficiency. The trigger and selection efficiencies were studied at various mass values by passing Monte Carlo samples through the same analysis chain as the real data. The trigger part of the simulation was cross checked against real data by comparing the simulation results with the trigger efficiency extracted from real events of a similar topology. The selection efficiency was found to vary from 34 % to

56 % as the mass difference between the squark and the LSP varied from 2 GeV to 6 GeV. For larger mass differences the efficiency decreases again since those events have more than 20 GeV of visible charged energy. The combined efficiency was parametrized as shown in Figure 4 and is known with an uncertainty of about 5 %.

The 95% confidence level search limits for 6 degenerate flavours, for a single flavour downtype and for a single flavour uptype from this method are shown labelled as A in Figure 5 a), b) and c), respectively.

5 Analysis and limits for light LSP

In the second analysis, which used a sample corresponding to 9300 hadronic Z^0 decays, two jet events were selected using the jet clusterization algorithm LUCCLUS [9]. The acoplanarity angle α_{xy} was calculated as the angle between the two jets projected on the plane perpendicular to the beam axis. The candidates were selected with the following criteria:

1. total visible charged energy larger than 15 GeV,
2. more than five charged particles,
3. $|\hat{z}| < 4$ cm,
4. $\sigma(z) < 6$ cm,
5. $|\cos(\theta_{thrust})| < 0.7$,
6. $\alpha_{xy} \leq 135^\circ$.

The first criterium was chosen in order to complement with some coverage the selection of Section 3.

After the selection the sample contained 31 candidates. For estimating the expected background from standard Z^0 decays, the Monte Carlo events described in Section 4 were used. It was found that 0.37 % of the simulated standard hadronic Z^0 decays satisfied the selection criteria, which corresponds to 34 ± 4 (stat.) events in the selected sample. The systematic error was estimated to be 10 % by comparing the distributions of the Monte Carlo events (with the parton shower fragmentation as well as with the string fragmentation) and the data in the variable $\alpha_{x,y}$. The background was subtracted from the number of candidate events, and a 5 % systematic error in the normalization was added in quadrature with the other errors. The result was -3 ± 7.5 events. The upper limit of 13 for the number of signal events satisfying the selection criteria was determined by excluding 95 % of the positive Gaussian probability density.

The detection efficiency for the squark signal was parametrized analogously to Figure 4, being typically 25 % for masses of the LSP up to half of the squark mass and for the squark masses larger than about $20 \text{ GeV}/c^2$. It was assumed to be known with about 5 % uncertainty.

The 95 % confidence level search limits based on this search are shown in Figure 5 labelled as B.

In conclusion, it is seen from Figure 5 that the combination of the two analyses exclude in the case of a LSP lighter than $20 \text{ GeV}/c^2$ three generations of squarks below $45 \text{ GeV}/c^2$, a single flavour downtype squark below $43 \text{ GeV}/c^2$ and a single flavour uptype squark below $42 \text{ GeV}/c^2$. For heavier LSPs (up to $m_{\tilde{q}} - 2 \text{ GeV}/c^2$) the limits extend to $44 \text{ GeV}/c^2$, $38 \text{ GeV}/c^2$ and $36 \text{ GeV}/c^2$, respectively. These results greatly improve the limits deduced from previous experiments, and are entirely new for the case of down type squarks.

After the completion of the present work a paper by the Mark II Collaboration was received [12] where similar conclusions are reached.

6 Acknowledgments

We are greatly indebted to our technical staffs, collaborators and funding agencies for their support in building the DELPHI detector and to the members of LEP Division for the speedy commissioning and superb performance of the LEP collider.

References

- [1] CELLO, Behrend H.-J. et al., *Z.Phys. C* 35 (1987) 181.
- [2] TOPAZ, Adachi I. et al., *Phys.Lett.* B218 (1989) 105.
- [3] UA1, Albajar C. et al., *Phys.Lett.* B198 (1987) 261.
- [4] CDF, F.Abe et al., *Phys.Rev.Lett.* 62 (1989) 1825.
- [5] UA2, Alitti J. et al., *Phys.Lett.* B235 (1990) 363.
- [6] H.Haber, G.Kane, *Phys.Rep.* C117 (1985), 75.
- [7] DELPHI detector, to be submitted to N.I.M.
- [8] A precise measurement of the Z^0 resonance parameters through its hadronic decays, DELPHI Collaboration, CERN-EP/90-32, submitted to *Physics Letters B*.
- [9] T. Sjöstrand, *Comp.Phys.Comm.* 27 (1983), 243; 28 (1983), 229, T. Sjöstrand and M. Bengtsson, *Comp.Phys.Comm.* 43 (1987), 367.
- [10] DELPHI, Aarnio P. et al. *Phys. Lett.* B240, (1990), 271.

[11] Particle Data Group, Phys. Lett. B204 (1988), 80-81.

[12] Mark II, T. Barklow et al., SLAC-PUB 5196, March 1990.

List of Figures

Figure 1: The distributions of total charged visible energy in the final state of squark pair production for various squark and LSP masses.

Figure 2: Efficiency of the DELPHI barrel track trigger used for this analysis as a function of the total visible charged energy.

Figure 3: Measured cross sections (corrected for the machine background) of events satisfying the selection criteria as a function of the center-of-mass-energy. The solid curve is the result of a two parameter fit of a Z^0 line shape plus a constant term both with a free normalization. The dashed curve corresponds to the 95 % C.L. upper limit.

Figure 4: Combined trigger and the selection efficiencies as a function of the squark mass and the LSP mass.

Figure 5: Extracted 95 % C.L. mass limits for scalar quark pairs decaying into LSP's for a) 6 flavours degenerate in mass, b) a single down squark, and c) a single up squark (right and left handed fields assumed degenerate in all cases). The limiting contours from the first and the second method are labelled as A and B , respectively. Also shown are limits from i) CELLO (95% C.L. single flavour) [1], ii) TOPAZ (95% C.L. single flavour) [2]. UA1 results[3] exclude $m_{\tilde{q}} < 45 \text{ GeV}/c^2$ (90% C.L. with five flavours) for $m_{LSP} < 20 \text{ GeV}/c^2$. CDF results [4] exclude $m_{\tilde{q}} < 74 \text{ GeV}/c^2$ (90% C.L. with six flavours) for $m_{LSP} < 30 \text{ GeV}/c^2$. UA2 results [5] exclude $50 < m_{\tilde{q}} < 74 \text{ GeV}/c^2$ (90% C.L. with five flavours) for $m_{LSP} < 20 \text{ GeV}/c^2$.

DELPHI

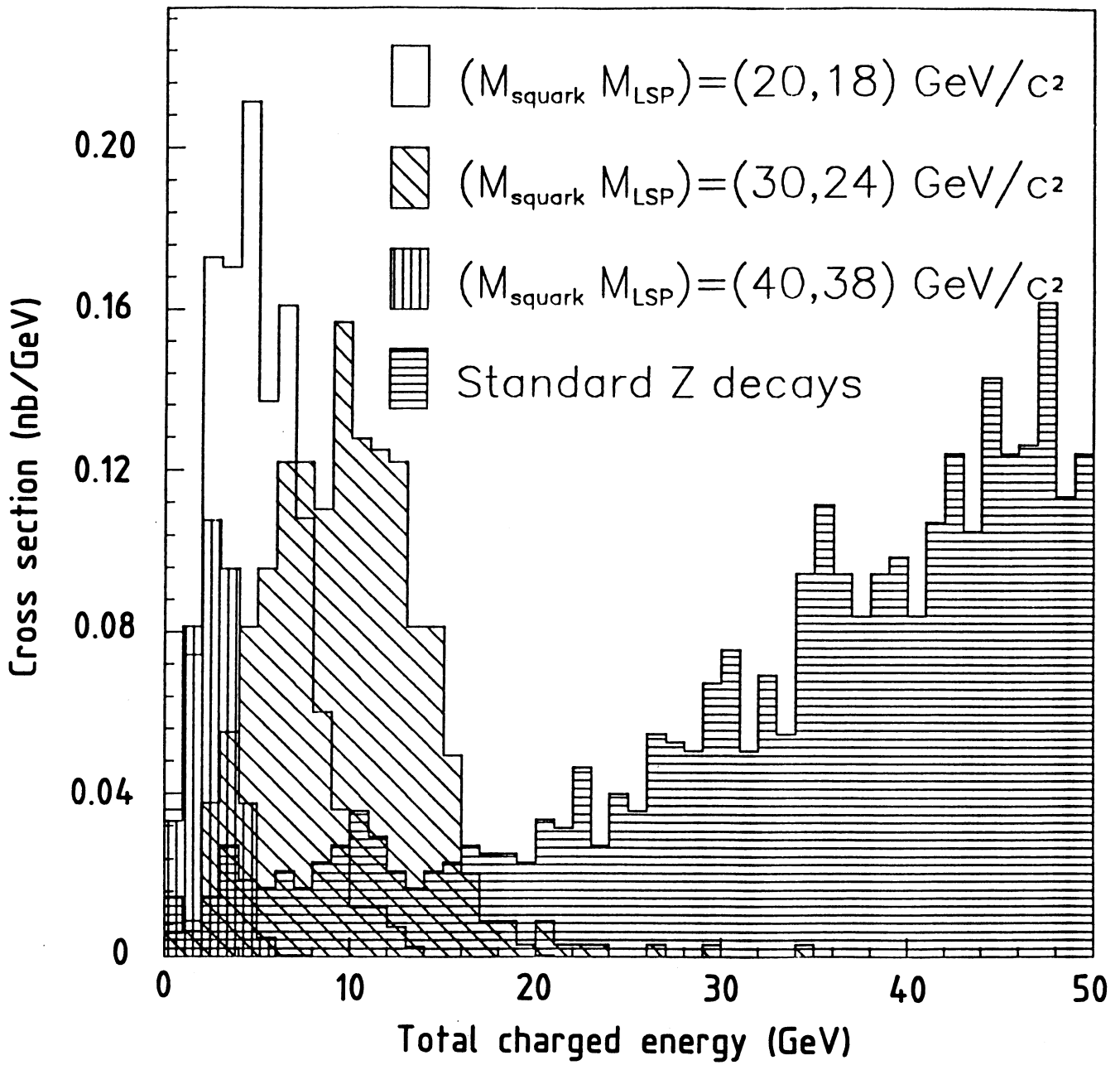


Fig. 1

DELPHI

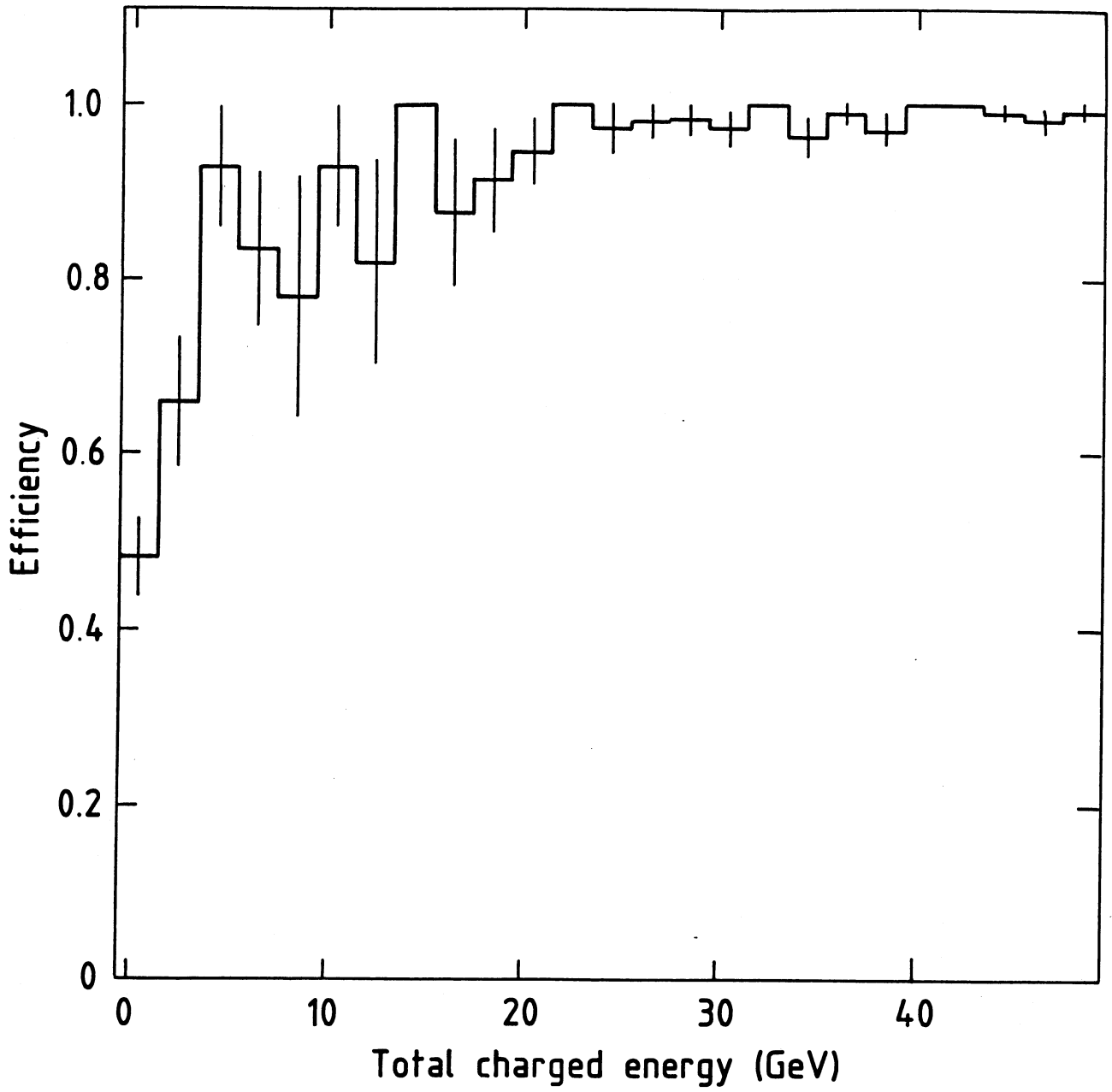


Fig. 2

DELPHI

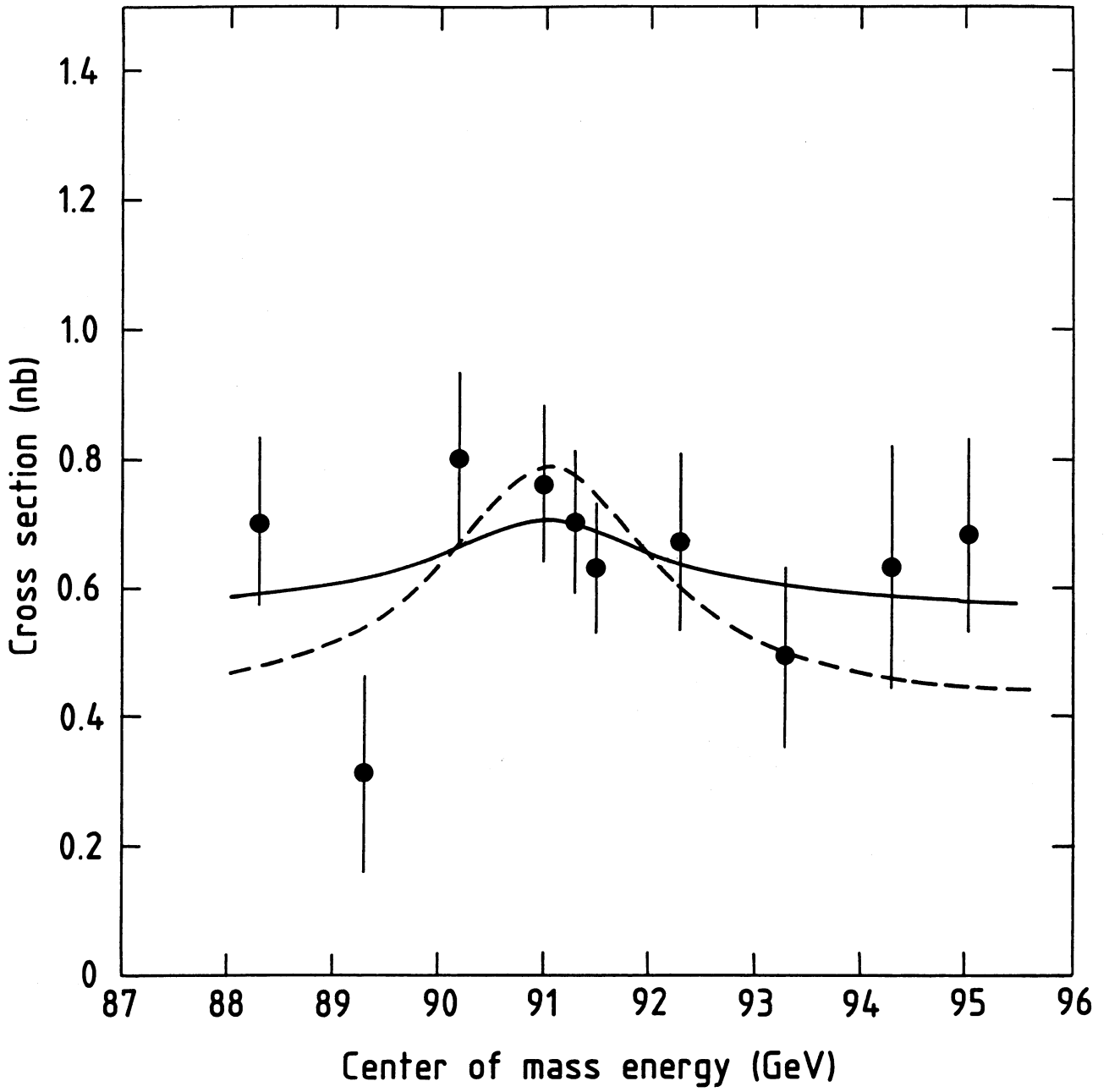


Fig. 3

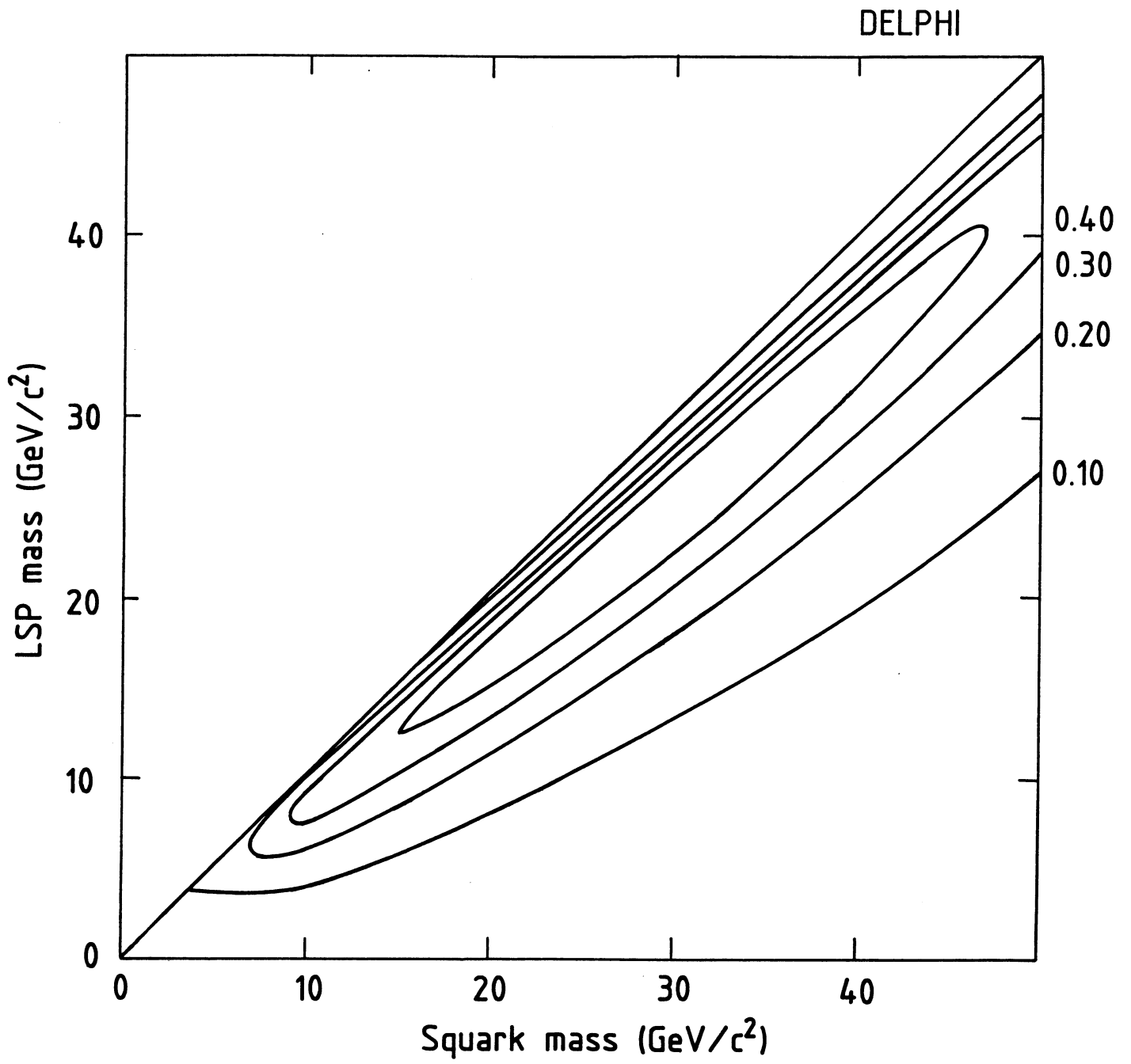


Fig. 4

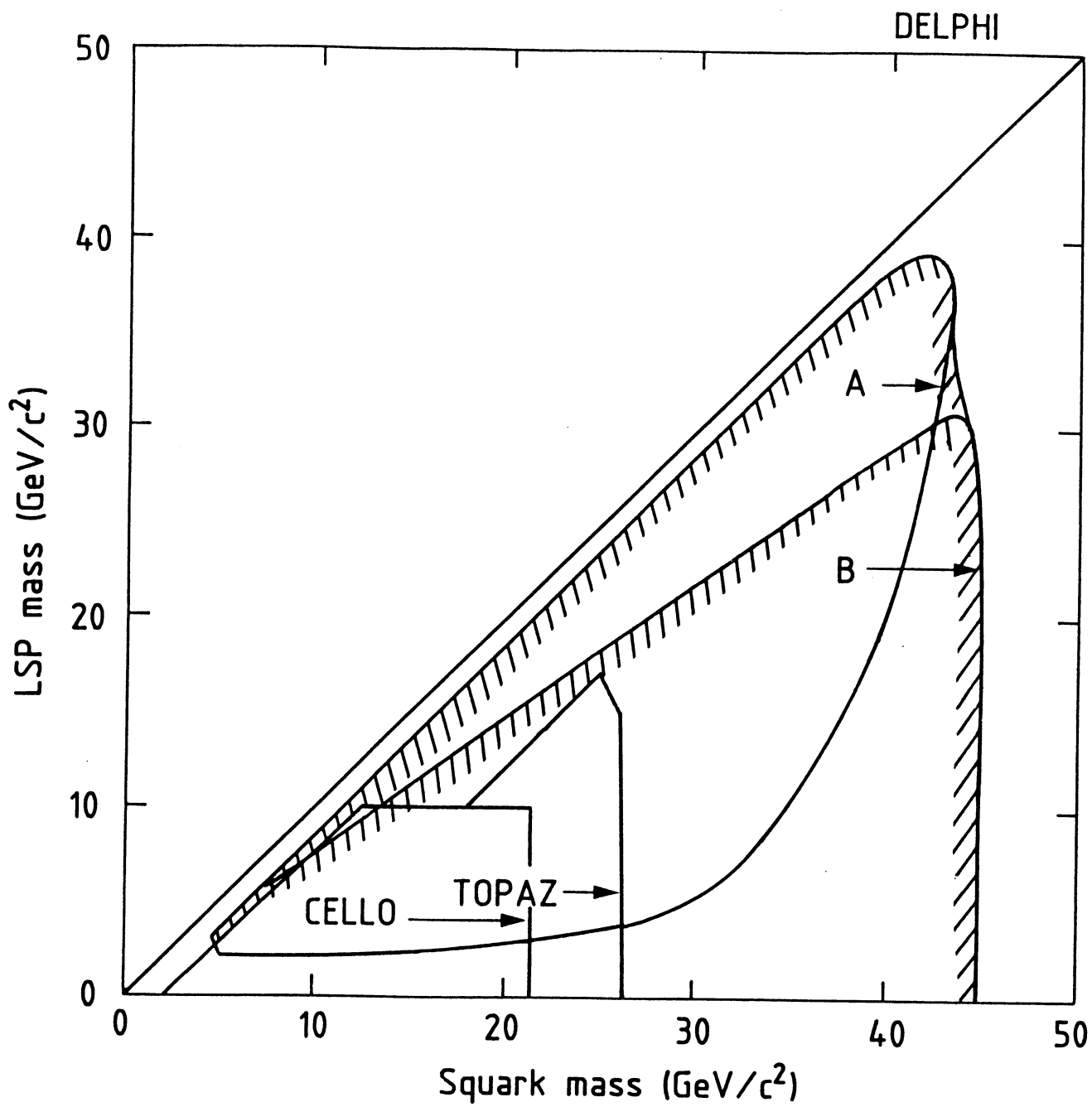


Fig. 5a

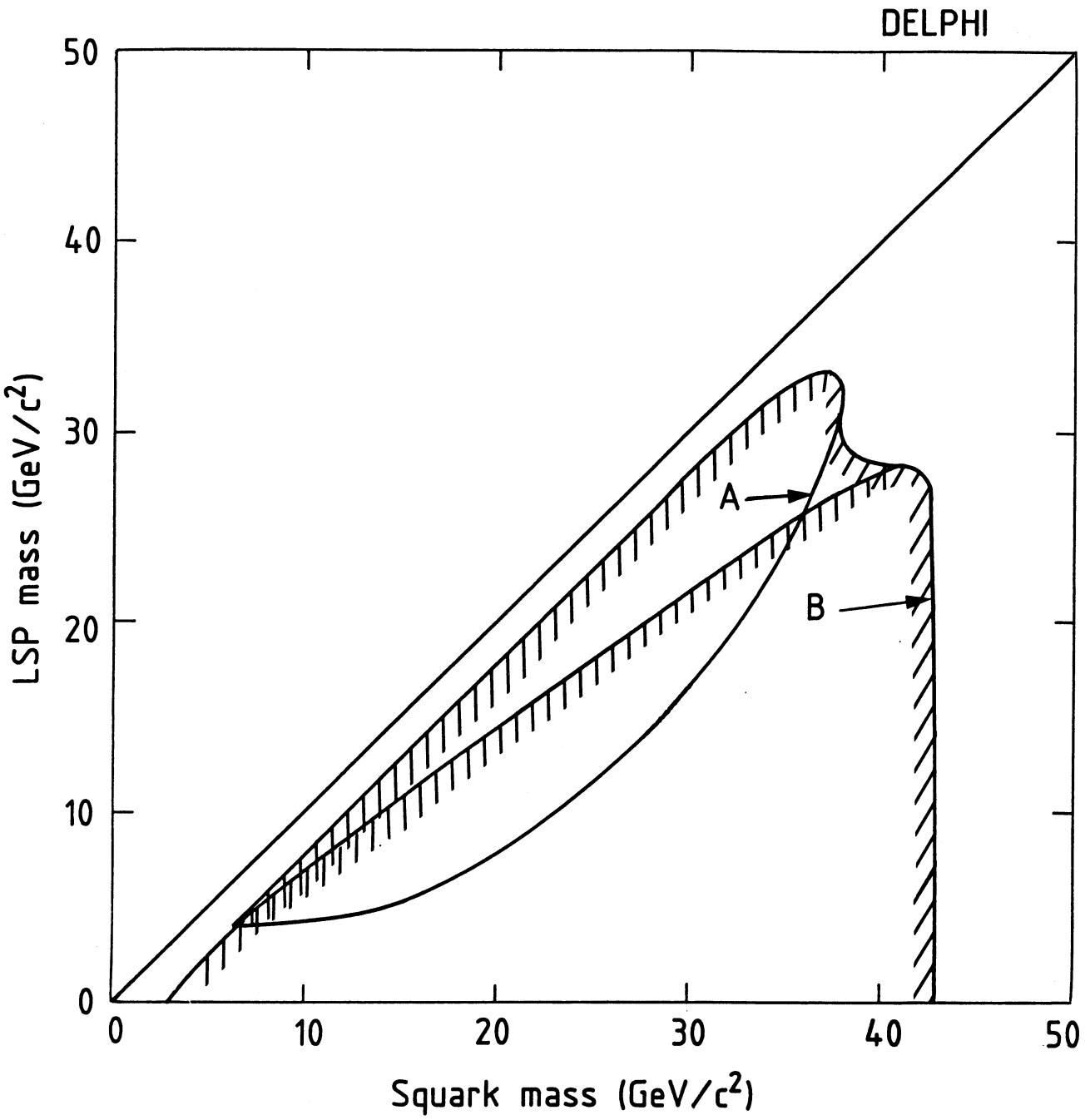


Fig. 5b

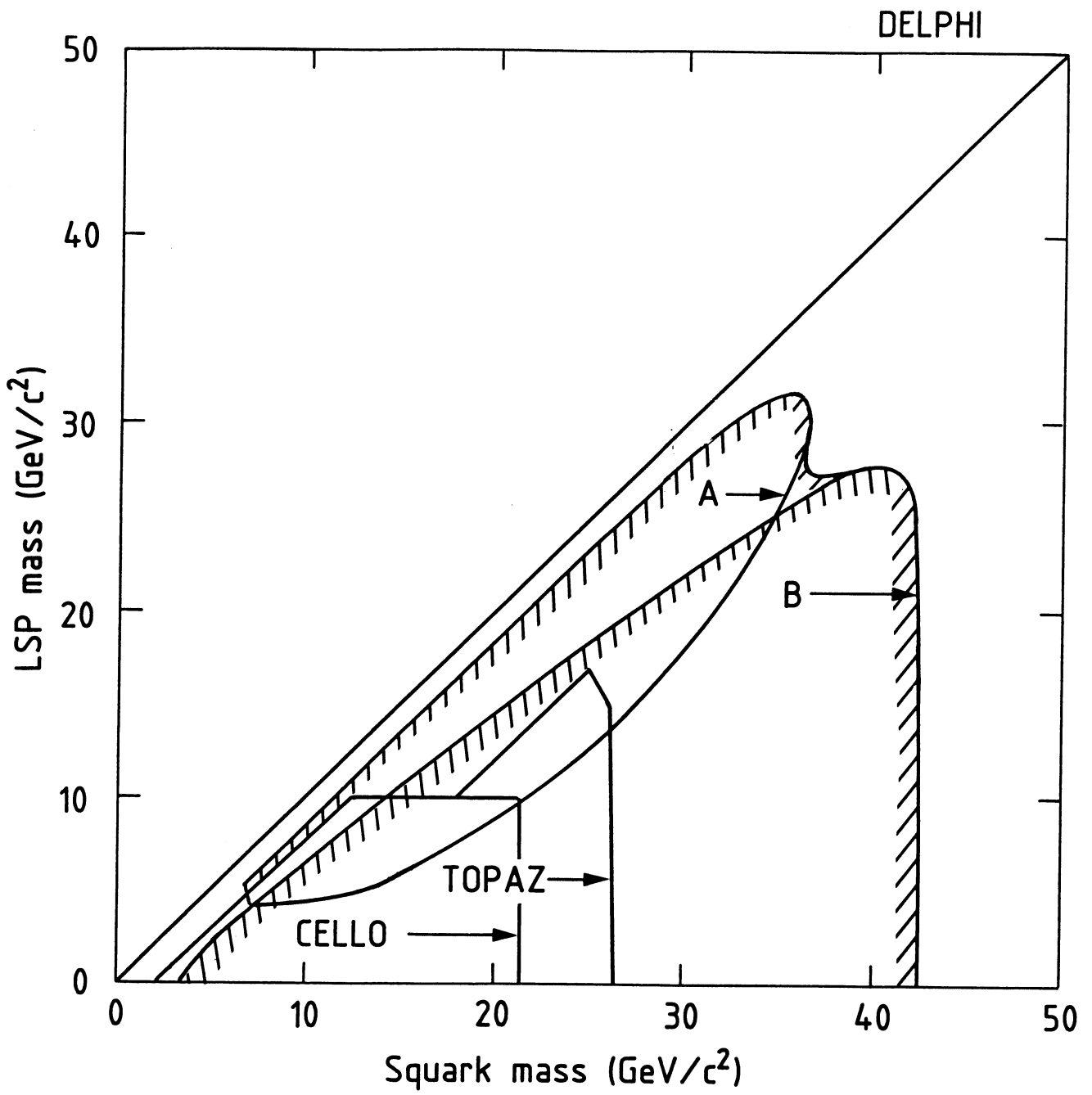


Fig. 5c